Research Article

Hussah M. Alobaid, Maha H. Daghestani, Nawal M. AL-Malahi, Sabah A. Alzahrani, Lina M. Hassen, and Dina M. Metwally*

Exploring the effect of silver nanoparticles on gene expression in colon cancer cell line HCT116

https://doi.org/10.1515/gps-2022-0094
received June 18, 2022; accepted November 08, 2022

Abstract: This study describes a new green method for silver nanoparticles (AgNPs) using *Cymbopogon proximus* (CP) extract and evaluates their potential anticancer properties in HCT116 cells. Ultraviolet-visible spectroscopy, transmission electron microscopy, dynamic light scattering, and Fourier transform infrared (FTIR) spectroscopy were used to successfully analyze the AgNPs. FTIR spectral analysis revealed the presence of phytochemicals that could be responsible for silver (Ag) ion reduction and AgNP capping. The 3-(4,5-dimethylthiazol-2-yl)-2,5-diphenyltetrazolium bromide assay demonstrated that treating HCT116 cells with PC-AgNPs for 48 h caused cytotoxic effects, as evidenced by the existence of 20% cell viability. The RT-qPCR study revealed that the expression of two oncogenes (cathepsin B [CTSB] and epithelial cell adhesion molecule [EpCAM]) was significantly reduced in treated cells. The levels of various tumor suppressor genes, including adenomatous polyposis coli (APC), Beclin1 (BECN1), nuclear translocation of β-catenin (CTNNB1), low-density lipoprotein receptor-related protein 6, LRP5, TP53, and TNF, were dramatically reduced in cells treated with CP extract, but this was not the case in cells treated with CP extract. To conclude, CP-AgNPs have demonstrated their ability to induce cytotoxic action and exert antitumorigenic modulatory effects, particularly on the expression of CTSB and EpCAM in colon cancer cells, utilizing AgNPs as an antitumor therapeutic agent for 48 h is not recommended, and reducing the treatment time could be more effective.

Keywords: silver nanoparticles, HCT116, *Cymbopogon proximus*

1 Introduction

Colorectal cancer (CRC) is a slow-developing cancer that begins as an abnormal tissue growth on the inner epithelial linings of large intestines [1,2]. If this growth becomes cancerous (polyp), it can form a tumor on the interior walls of the colon or rectum [1]. Subsequently, this tumor will grow into blood vessels or lymph vessels, increasing the chance of metastasis to other anatomical sites [2]. CRC is considered the third most lethal cancer worldwide [3,4], representing the fourth most happening malignancy among all ages and for men and women combined [3,4]. According to Saudi Cancer Registry in Saudi Arabia (KSA), CRC has been ranked first in incidence among Saudi males and third among Saudi females for the last several years. The rate among males was 19.3%, and among females was 9.2% [5]. Although the cases of CRC in KSA are lower when compared to the western population, it seems to be increasing during the past few years [6–8].

Most CRC originates because of multifactorial causes; however, the interaction between genetic and environmental factors plays the most significant role. It can be attributed to the increasingly aging population, unfavorable modern dietary habits, and increased risk factors such as smoking, alcohol consumption, high-fat diet, low physical exercise, and obesity [9]. Risks are dramatically increased for individuals who inherit the gene mutations responsible for familial adenomatous polyposis or hereditary nonpolyposis CRC [7,10].

Approximately 85% of CRC have a mutation in multiple genes. These are adenomatous polyposis coli (APC), tumor protein 53 (TP53) [11], Beclin1 (BECN1), and epithelial cell adhesion molecule (EpCAM) [12]. Studies showed that the loss of function of the APC gene interacts with the CTNNB1 (nuclear translocation of β-catenin) [13].

* **Corresponding author: Dina M. Metwally,** Department of Parasitology, Faculty of Veterinary Medicine, Zagazig University, Zagazig, Egypt, e-mail: mdbody7@yahoo.com
Hussah M. Alobaid, Maha H. Daghestani, Nawal M. AL-Malahi, Lina M. Hassen: Department of Zoology, College of Science, King Saud University, Riyadh, 11495, Saudi Arabia
Sabah A. Alzahrani: Department of Biochemistry, College of Science, King Saud University, Riyadh, 11495, Saudi Arabia

This interaction leads to triggering the Wingless-related integration site (Wnt signaling pathway). These findings directly link Wnt signaling and human CRC [14–16]. An important co-receptor of the Wnt pathway is low-density lipoprotein receptor-related protein 6 (LRP6), which forms a signalosome along with a Wnt ligand to activate the downstream signaling pathway [17]. According to the previous study, LRP6 contributes to the progression of CRC and certain other cancers [18]. In CRC, however, the mechanism underlying LRP6 is rarely investigated. Tumor formation and metastasis are influenced by BECN1. A marked increase was observed in the motility and invasion of CRC cells when BECN1 was knocked down. BECN1 negatively regulates CRC metastasis in an autophagy-independent manner through STAT3 signaling pathway activation. Potential therapeutic targets for metastatic CRC include the BECN1/Janus kinase 2 (JAK2)/signal transducer and activator of transcription 3 (STAT3) signaling pathway [19]. In normal cells, cathepsin B (CTSB) is a peptidase that functions in endo-lysosomal compartments [20]. CTSB production can be altered at multiple levels during malignant transformation, resulting in the overproduction of the enzyme, which plays a crucial role in several pathologies and oncogenic processes [21]. A malignant transformation of tumor cells can alter the regulation of CTSB at multiple levels, resulting in enhanced local release [21,22]. In theory, CTSB may be used to treat and chemoprevention of neoplasms and molecular detection [23]. A previous study demonstrated that human CRC cells treated with Ca074 showed enhanced invasiveness after being treated with the highly selective and non-permeant cathepsin B inhibitor [22]. Studies also demonstrated that CRC is associated with overexpression in a tumor-suppressive protein (EpCAM) [12].

CRC survival rates remain below 10% despite new treatments. Consequently, many research efforts are devoted to understanding metastasis, identifying biomarkers, and developing therapeutic targets for CRC [24]. Researchers and clinicians have developed various methods to prevent or inhibit cancer growth in the last three decades. The common types of cancer treatment are surgery, chemotherapy, radiotherapy, immunotherapy, hormone therapy, and photodynamic therapy. Despite the progress in our knowledge about cancer, current strategies for cancer treatment are not very effective. For instance, chemotherapy and radiotherapy damage the cancer cells and other healthy cells in the body [25]. FOLFOX is the most successful standard chemotherapy treatment for CRC [26], despite that, it has severe side effects (e.g., gastrointestinal and neurotoxicities) [26]. Thus, scientists are still trying to find a new biocompatible and more effective method for cancer treatment using nanotechnology and natural products.

Nanotechnology is an important field of modern research dealing with particle structure design, synthesis, and manipulation [27]. In recent years, silver nanoparticles (AgNPs) have drawn more attention to their significant biological role against microorganisms [28]. It was found that AgNPs exhibited both positive and negative effects on well-developed multi-organ systems, including humans and rats. However, the general consensus states that capped (bio)molecules have synergistic bioactivities and can reduce its toxicity. Yet, there is no convincing evidence to support this claim [29,30]. These particles have a considerable surface area compared to raw silver particles ranging from 1 to 100 nm in one dimension. This feature could provide promising and novel chemical property in their nanoscale size [26,29]. The AgNPs are the most commercialized and prominent group of nano-compounds due to their diverse applications in the health sector [30]. These particles can be prepared easily by different chemical, physical, and biological approaches [31]. However, the biological approach is the most emerging approach to preparation. This is because it is easier, cost-effective, eco-friendly, and less time-consuming and does not involve any toxic chemicals as other methods [31,32].

Combining AgNPs with plant extracts can result in AgNPs with better characteristics. This is due to the synergistic action of both AgNPs and the bioactive compounds found in plants. As a result, plant-mediated AgNPs are more physiologically active than standard AgNPs [33,34]. Several medicinal herbs have been used to synthesize AgNPs. *Cymbopogon proximus* (CP) (Gramineae) is a herbal plant, commonly known as "camel's hay" and locally as Maharaib, Halfa-bar Sakhbar, or Athkhar [34–36]. CP is widely distributed in the Middle East, Africa, temperate Asia, western Asia, and tropical Asia [37]. CP plant is traditionally used as an addition to tea, diet, and medicine. The medicinal properties of CP grass are to treat intestinal spasms, stomach disorders, bowel irritation, dyspepsia, and diarrhea [35,37]. The most important active compounds of CP are terpenes and saponins, which have cancer chemopreventive effects, antimicrobial, antifungal, antiviral, antihyperglycemic, anti-inflammatory, and anti-inflammatory antiparasitic activities [38].

This study aimed to characterize the green-synthesized AgNPs from the CP extract using ultraviolet-visible (UV-Vis) spectroscopy, transmission electron microscopy (TEM), dynamic light scattering (DLS), and Fourier transform infrared (FTIR) techniques and, then, assess its potentiality to be anticancer by studying the cytotoxic effects of CP extract and CP-AgNPs and the expression levels of oncogenes APC, BECN1, CTNNB1, LRP6, LRP5,

tumor necrosis factor (TNF), tumor protein 53 (TP53), CTSB, and EpCAM on CRC cell line (HCT116).

2 Materials and methods

2.1 Plant extract preparation

Fresh grasses of CP were collected from a local market. Around 10 g of the plant was thoroughly washed with sterile double distilled water two to three times until all impurities were removed. They were then boiled for 20 min in 150 mL of distilled water and left to be cooled at room temperature overnight. Then, they were filtered and stored at 4°C until required for further analysis (Figure 1a).

2.2 Synthesis of AgNPs

Five milliliters of aqueous plant extract prepared above were added to 50 mL of 1 mM of aqueous silver nitrate solution ($AgNO_3$). The reaction mixtures were stirred under a vigorous stirrer with heat for 3–5 h (at 80°C). The change in the reaction mixtures was monitored to determine the nanoparticle formation (Figure 1b).

2.3 Characterization of AgNPs

The synthesized leaf extract AgNPs were characterized using different techniques detailed subsequently.

The UV-Vis spectrophotometer (PerkinElmer LS 40, USA) was used to evaluate the formation of AgNPs at wavelengths ranging from 300 to 600 nm (Figure 1c). The morphology and average size of the synthesized AgNPs were determined by TEM (Figure 2). The TEM images of synthesized AgNPs were obtained using a JEOL JEM-2100 (JEOL Ltd., Tokyo, Japan) high-resolution TEM operated at an accelerated voltage of 200 kV. An electron beam is imaged in this method while it passes through a thin sample (less than 100 nm). A detector is then used to visualize objects smaller than a nanometer based on the transmitted beam. Before analysis, AgNPs were sonicated for 5 min, and a drop of appropriately diluted sample was placed onto a carbon-coated copper grid. The liquid fraction was allowed to evaporate at room temperature. The hydrodynamic size and zeta potential of the synthesized CP-AgNPs were measured by the DLS technique using a zetasizer device (Malvern, Worcestershire, UK; Figure 3).

Further characterization was done using FTIR (Nicolet 6700, FTIR, Thermo Scientific, Waltham, MA, USA) spectral measurements to detect the functional group responsible for reducing ions to AgNPs. This was done by mixing 300 µL of the air-dried AgNPs with 10 mg potassium

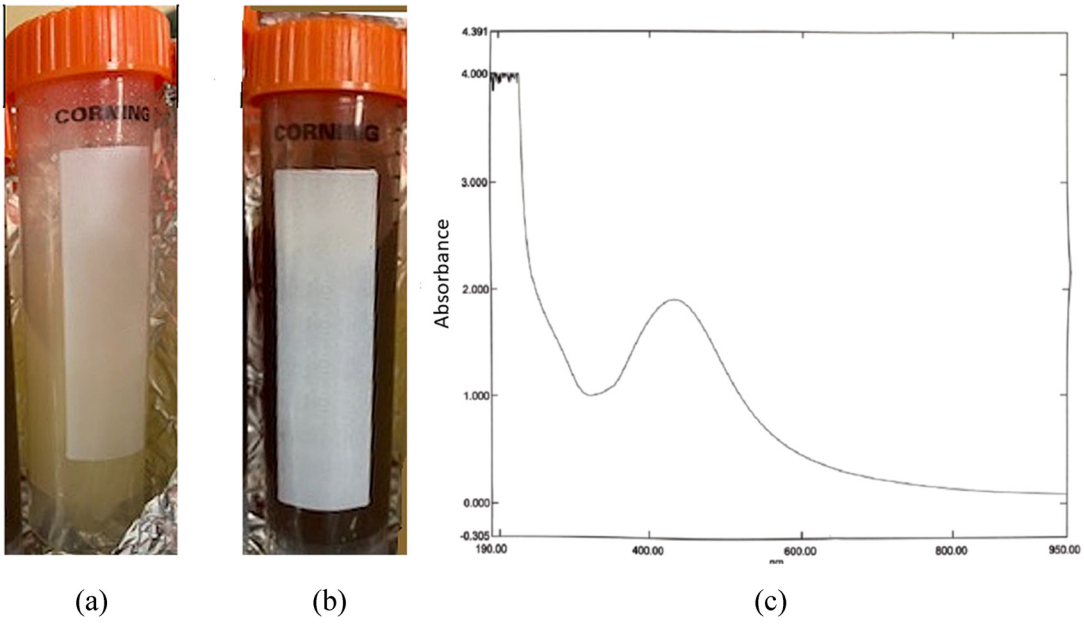

Figure 1: The green synthesis of AgNPs: (a) the aqueous plant extract. (b) Mixture of $AgNO_3$ with aqueous extraction of CP. (c) Characterization of AgNPs using the UV-Vis spectroscopy.

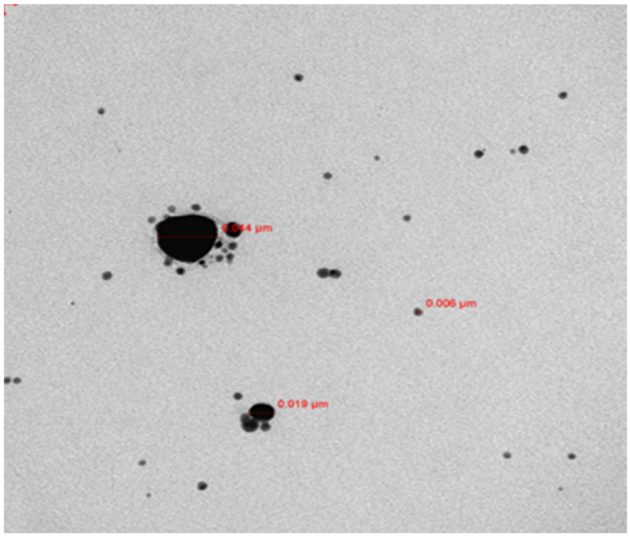

Figure 2: TEM image of nanoparticles. A graph of a TEM image of AgNPs at a magnification level of 100 nm.

bromide and then oven dried. The FTIR spectra were taken at the range of 500–4,000 cm^{-1} and a resolution of 4 cm^{-1}.

2.4 Cell culture preparation

A human colorectal carcinoma cell line (HCT116) was commercially bought from American Type Culture Collection. The cells were routinely cultured in Dulbecco's modified Eagle's medium, 10% heat-inactivated fetal bovine serum, 100 $U{\cdot}mL^{-1}$ penicillin, 0.1 $mg{\cdot}mL^{-1}$ streptomycin, and 1% glutamine. The cells were seeded in 96-well plate at a 2×10^5 $cell{\cdot}well^{-1}$ density in 100 µL of optimized medium and incubated at 37°C and 5% CO_2. The total number of cells used in the different experiments was determined by the trypan blue exclusion test (0.4%) using a cell counter.

2.5 Cytotoxicity assay

The cytotoxicity of synthesized AgNPs against HCT116 cells was measured by the 3-(4,5-dimethylthiazol-2-yl)-2,5-diphenyltetrazolium bromide (MTT) assay (kit from UFC Biotechnology). After culturing the cells, they were allowed to settle for 24 h before being treated with an individual concentration of CP extract and synthesized CP-AgNPs (3.125, 6.25, 12.5, 25, 50, and 100 µL). Treated cells were allowed to grow further for 48 h. At the end of the incubation period and concentration point, 100 µL of 0.22 µm filter-sterilized MTT (Sigma Aldrich, UK) was added at 37°C at a final concentration of 5 $mg{\cdot}mL^{-1}$. The 96-well plate was kept in the dark for 2 h before the medium containing MTT was removed. One hundred microliters of dimethyl sulfoxide (Ajax Finechem Pty Ltd, Australia) were added to dissolve formazan crystals. The 96-well plate was also shaken for 15 min in the dark to help dissolve the formazan crystals. Each treatment's optical density (OD) was measured at an absorbance of 490 nm using a 96-well plate reader (Molecular Devices – SPECTRA max – PLUS384). Each experiment was performed in four replicates. Values of OD were normalized according to the control (untreated cells). Therefore, cell viability values of untreated cells should be 100%, while values of treated cells are below or above 100%.

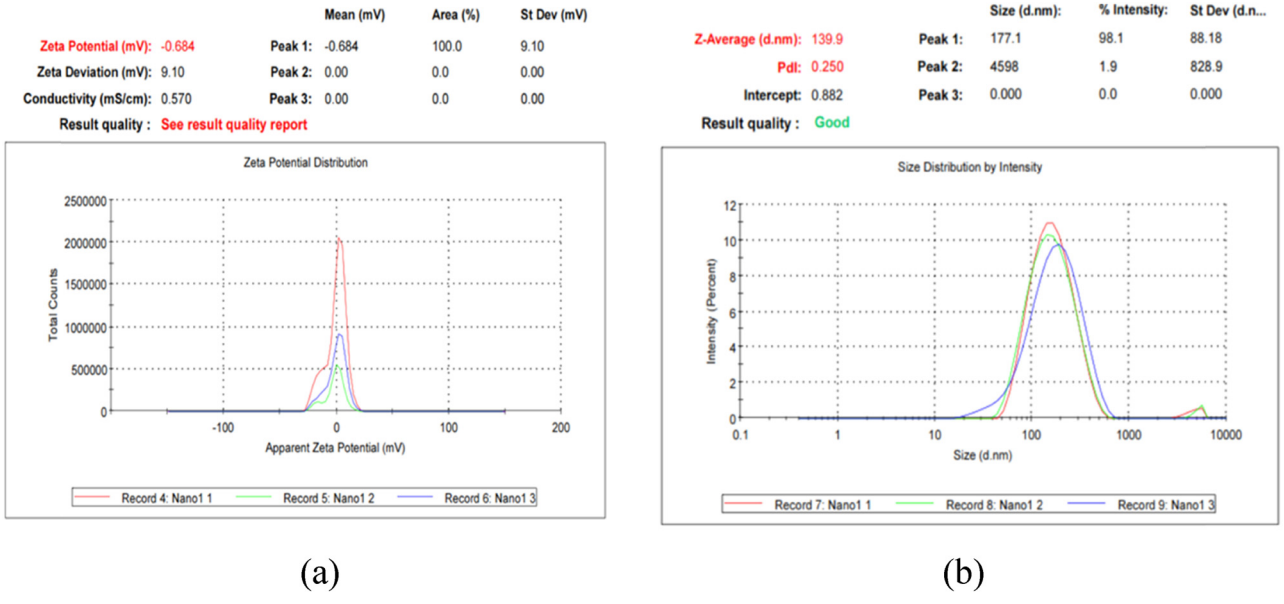

Figure 3: DLS measurement reveals the zeta potential value of CP-AgNPs (a) and hydrodynamic size (b).

2.6 Total RNA extraction and cDNA synthesis

A high-capacity cDNA reverse transcription kit (Applied Biosystems, Thermo Fisher Scientific, USA) was used to perform reverse transcription in the Veriti 96 Well Thermal Cycler. Cultured cells at a density of 2×10^5 cells·well^{-1} in six-well plates were treated with different concentrations of CP extract as crude and CP-AgNPs for 48 h. Then, the total RNA was extracted following the RNeasy Plus Mini kit (Qiagen). The purity and quantity of total RNA were measured using NanoDrop Spectrophotometer (Thermo Scientific), and its integrity was examined using the gel agarose electrophoresis, as detailed here [39].

2.7 Real-time polymerase chain reaction (RT-PCR)

For the genetic evaluation of the effect of CP-AgNPs, the expression levels of APC, CTNNB1, BECN1, CTNNB1, LRP6, TNF, CTSB EpCAM, and TP53 were determined using RT-PCR. It was performed by QuantiTect SYBR Green PCR Kit (Qiagen, Cat # 204143, USA) and the Applied Biosystems ViiA7 (Life Technologies), and the instruction manual of Real-Time-Gene was followed. β-Catenin gene is mutant in HCT116 [40].

2.8 Statistical analysis

The Statistical Package for the Social Sciences (SPSS) software (version 20.0) was used for data obtained from particle size analysis and cell availability assay. ANOVA and *t*-test were used to analyze the differences between the groups, and $p < 0.05$ was considered significant. For each parameter, mean ± SD for at least three independent experiments was calculated.

3 Results

3.1 Characterization of AgNPs with CP

The formation of synthesized CP-AgNPs is presented in Figure 1. The colorless solution of $AgNO_3$ turned dark brown after being mixed with the yellow aqueous extract of CP within 24 h. An examination of the UV-Vis spectrum reveals a significant peak value at 432.5 nm (shown in Figure 1b). The shape and size of AgNPs were determined by the TEM and shown to be predominated by spherical-shaped morphologies (Figure 2). They ranged from 6 to 44 nm with an average size of 21.2 nm. The small relative size of CP-AgNPs indicates their nanocrystalline nature. This, in turn, supports their high catalytic and accumulation properties in the tumor area [41]. The formation of monodispersed particles was confirmed by measuring the hydrodynamic size of CP-AgNPs via zetasizer. As shown in Figure 3a, the zeta potential value was −0.684 mV, and its size was 139.9 diameter value of nanometer with 0.250 PDI (Figure 3b). The functional biomolecules in the CP extract were identified using FTIR spectral measurements in a wavelength range of 4,000–400 cm^{-1}. These biomolecules are responsible for the reduction of the bio-reduced AgNPs. As shown in Figure 4, the pattern of peaks of both CP and CP-AgNPs reveals the binding of the silver ion with carboxylic and amide groups of CP, and the multiple peaks represent its complicated nature.

3.2 MTT assay

This test was conducted to assess the percentage of viable cancer cells treated with different concentrations of PC as either AgNPs or crude for 24 h of the control sample (100%) (Figure 5). The present study obtained the minimum inhibitory concentration (IC_{50}) of AgNPs on the experimental cells at 25 µL. Exposure to increasing concentration of AgNPs exhibits significant dose-dependent anticancer activity in CRC cells. As shown in Figure 5, both crude and AgNPs significantly reduced the number of cancer cells, but the effect of AgNPs was more significant than the effect of the crude (compare Figure 5a and b).

3.3 RT-PCR

The expression levels of the indicated genes were measured in HCT116 cells using quantitative RT-PCR. The cells were treated with 6.25 µL of CP aqueous extract and 25 µL of synthesized CP-AgNPs for 48 h. Results showed that the expression level of APC, BECN1, CTNNB1, TNF, and TP53 was abrogated entirely in cells treated with NPS ($p \leq 0.05$), whereas cells treated with the crude significantly increased the levels of both APC and CTNNB1 compared to the control ($p \leq 0.05$) (Figure 6a–e). In the same way, treating cells with NPs inhibited remarkably the expression level of both LRP6 and LRP5 (Figure 6f and g). However, the inhibition was significant in the former ($p \leq 0.05$) and non-significant in

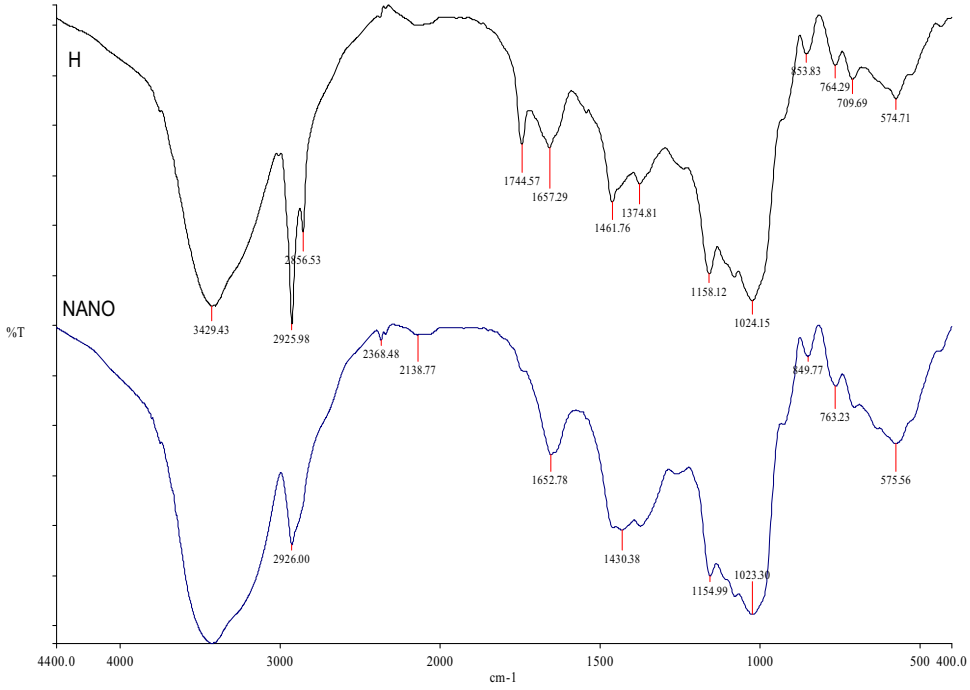

Figure 4: The spectra of AgNPs were recorded in the wavelength range of 4,000–400 cm^{-1} via FTIR.

the latter, despite the reduction being around ~30% ($p > 0.05$). The CTSB and EPCAM genes are shown in Figure 6h and i that treating cells with 6.25 µL-CP aqueous extract or 25 µL-synthesized CP-AgNPs has induced a downregulation effect ($p < 0.05$) by suppressing the expression level of both genes.

4 Discussion

There has been a tremendous interest in using AgNPs as a drug carrier, cancer treatment, nanotechnology, and the field of biomedicine [42]. AgNPs' synthesis strategies have evolved in the past few decades to develop eco-friendly and cost-effective synthesis methods [42–44]. This study developed a nano-drug using CP and assessed its anticancer activity against CRC cells (HCT116). The changing color of $AgNO_3$ solution within 15 min indicates the reduction of the Ag ion to AgNPs. Furthermore, we applied multiple methods to evaluate the formation of green synthesis of AgNPs. The UV-Vis spectroscopy revealed a strong absorption peak at 432.5 nm of the CP-AgNPs, the highest absorbency due to their reduced $AgNO_3$ content, and surface plasmon resonance [45]. The TEM images validate the spherical shape of CP-AgNPs,

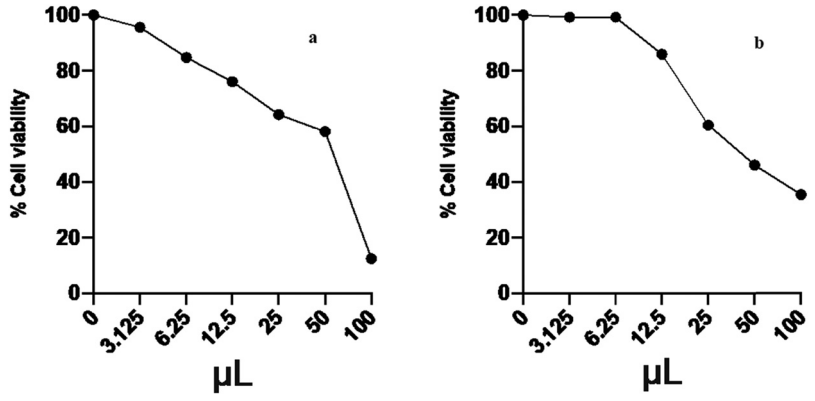

Figure 5: Impact of various concentrations of CP-AgNPs (a) and plant extract (crude) (b) on the cell viability in HCT116 cells.

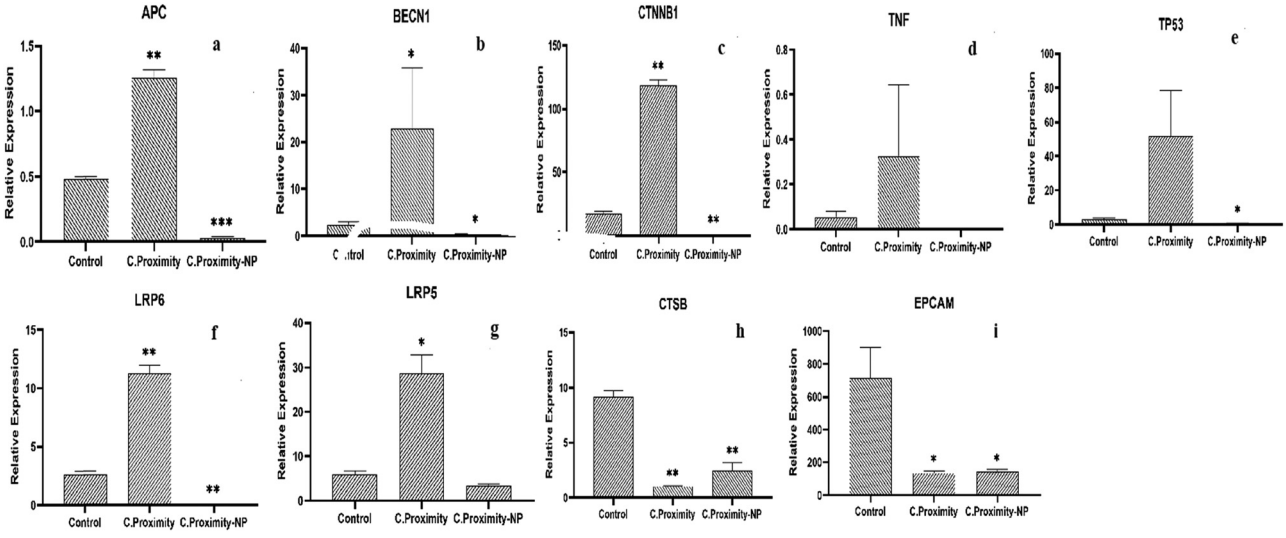

Figure 6: The expression levels of (a) APC, (b) BECN1, (c) CTNNB1, (d) TNF, (e) TP53, (f) LRP6, (g) LRP5, (h) CTSB, and (i) EPCAM.

and they have an average size of 21.2 nm. A significant aggregation of the nanoparticles was also observed. This could have been caused by the coating (capping agents) that covers the NPs. This causes the NPs to be attached, resulting in a decreased space between the NPs [46,47]. The FTIR confirmed that the proteins bind to the metal NPs strongly that they form a coating on the AgNPs. The DLS results indicate variation in dimensions of AgNPs. Therefore, the results suggest that the CP extract may serve a dual purpose by forming and stabilizing AgNPs in aqueous solutions.

CRC is a heterogeneous disease caused by genetic and epigenetic alterations in cells, transforming from an adenoma to carcinoma. Globally, it is ranked second as the most frequent type of cancer-related mortality [48]. To the best of our knowledge, no study has examined the chorionic effect of this extract on CRC in the form of NPS. The cytotoxic study suggested a proliferative effect of PC extract as crude and PC-AgNPs against cancerous cells (HCT116) (Figure 5). The observed effect of AgNPs could be linked to their capacity to activate reactive oxygen species in cells, triggering oxidative stress (OS), or related to modulation by autophagy and thereby causing cell death [49,50]. A growing number of studies highlight the significant impact of AgNPs in inducing a dose-dependent cytotoxicity effect in LoVo cells (a large intestine cell line) [41] and in HCT116 cells (a colon cancer cell line), which were treated with AgNPs of naringenin [51] or *Chaetomorpha linum* for 24 h [52]. Moreover, leaves and extracted oil have been reported to have antioxidant activity, which may explain the observed activity in the cancer cell lines [35].

The analysis of molecular studies showed a significant alteration in the expression levels of oncogenes in treated cancer cells compared to the control. The results herein showed that the effect of the plant extract as crude was more efficient than NPs in enhancing these genes. Indeed, treating cells with PC-AgNPs abrogate the expression levels of APC and other genes that are associated with, such as BECN1, CTNNB1, LRP6, LRP5, TNF, and TP53.

On the other hand, PC crude significantly promotes the expression levels of APC, BECN1, CTNNB1, LRP6, LRP5, TNF, and TP53 and works as anticancer activity (Figure 6). These findings are somewhat surprising because PC extract (crude) and PC-AgNPs have proliferative effects on cell viability (Figure 5). Moreover, researchers previously investigated the effect of AgNPs on cells like CRC and found a positive result [52]. The differences between our work and their work are that they treated cells for 24 h and here for 48 h. The time length could lead to a passive accumulation of NPs. The acute treatment could have a reverse effect [50,53]. Kermanizadeh et al. demonstrated that giving rats one dose of AgNPs did not affect healthy liver functions, but severe dysfunctions can be observed after an acute dose of AgNPs [54]. Thus, how AgNPs accumulate may affect the function of these organs and cells, as these partials can produce OS and free radicals [50].

Furthermore, the harmful effects of AgNPs treatments were reported to induce neurotoxicity in the brain [55] and altered gene expression profiles [56], cross the blood–brain barrier, and even change the animal behavior [57]. The size should also be considered, which is another possible explanation for these unexpected results. It was reported that the best size should range

between 10 and 100 nm, and here, the average size is 20 nm. This smaller size with the length of the treatment may contribute to a massive accumulation exhibiting toxic impact.

On the contrary, both CTSB and EpCAM genes are overexpressed in colon cancer. CTSB functions primarily as an endopeptidase in endolysosomes [22]. When tumors expand, CTSB can be overexpressed and exported outside the cells, as the regulation of the protein is altered at multiple levels [22]. According to this, CTSB might play a role in alterations contributing to cancer progression. EpCAM is a tumor antigen and serves as a prognostic indicator. Besides that, it is also a therapeutic target and a molecule anchoring in circulating and disseminated tumor cells. It is considered a multi-functional transmembrane protein that regulates the adhesion, proliferation, and migration of carcinoma cells [58]. Results herein demonstrated that both CP crude and CP-AgNPs had a modulatory effect on the levels of these genes in CRC cells (Figure 6). It is suggested that the PC-AgNPs have anticarcinogenic modulatory effects. Noteworthy, considering the importance of the Wnt/APC/CTNNB1 pathway in initiating human tumorigenesis, our data emphasize the association between the overexpression of CTSB and the mutation of APC. This is in line with previous work that clarified that CTBS could deregulate the mutation of APC, leading to the insufficient breakdown of CTNNB1 and increased nuclear signaling [59].

5 Conclusion

The present study has efficiently synthesized AgNPs using CP. The doses were 6.25 and 25 µL of PC crude and AgNPs, respectively. HCT116 cells were treated for 48 h and exhibited a cytotoxic effect on the growth of CRC. However, the PC-AgNPs have had a negative impact on oncogenes levels. In contrast, the CP crude significantly enhanced the mutant genes (tumor suppressor). It does not mean that utilizing AgNPs is an ultimately harmful tool. It could be related to the long period of treating cells, and it is advisable to repeat the work by treating cells for 24 h before concluding. In addition, PC-AgNPs have deactivated both CTSB and EpCAM. Overall, we can conclude that this study highlights the great potential of AgNPs to be used as a nontoxic anticancer drug delivery system, considering the length of treatment which could minimize the negative impact on cells.

To sum up, this technique is a double-edged sword, mainly applied to highly heterogeneous cells. Cancer cells are unique in their behavior. Same cells with the same tumor could have different genetic changes and could act differently to the exact therapy. Still, further investigations are needed to optimize the best size and treatment period for each type of cancer.

Funding information: This research project was supported by Researchers Supporting Project number (RSP-2022/R495), King Saud University, Riyadh, Saudi Arabia.

Author contributions: Hussah Alobaid: writing – original draft, writing – review and editing, formal analysis; Maha Daghestani: designed the experiment and funding resources; Nawal Almelahi: carried out the gene expression; Sabah A. Alzahrani and Lina M. Hassen: formal analysis of gene expression; Dina M. Metwally: writing – review and editing.

Conflict of interest: Authors state no conflict of interest.

Data availability statement: All data generated or analyzed during this study are included in this published article.

References

[1] Testa U, Pelosi E, Castelli G. Colorectal cancer: genetic abnormalities, tumor progression, tumor heterogeneity, clonal evolution and tumor-initiating cells. Med Sci. 2018;6(2):31.
[2] Valastyan S, Weinberg RA. Tumor metastasis: molecular insights and evolving paradigms. Cell. 2011;147(2):275–92.
[3] Bray F, Ferlay J, Soerjomataram I, Siegel RL, Torre LA, Jemal A. Global cancer statistics 2018: GLOBOCAN estimates of incidence and mortality worldwide for 36 cancers in 185 countries. CA Cancer J Clin. 2018;68(6):394–424.
[4] Erratum: Global cancer statistics. GLOBOCAN estimates of incidence and mortality worldwide for 36 cancers in 185 countries. CA Cancer J Clin. 2018;70(4):313.
[5] Alqahtani WS, Almufareh NA, Domiaty DM, Albasher G, Alduwish MA, Alkhalaf H, et al. Epidemiology of cancer in Saudi Arabia thru 2010–2019: a systematic review with constrained meta-analysis. AIMS Public Health. 2020;7(3):679–96.
[6] Mosli MH, Al-Ahwal MS. Does the increasing trend of colorectal cancer incidence in jeddah reflect a rise in the Kingdom of Saudi Arabia? Asian Pac J Cancer Prev. 2012;13(12):6285–8.
[7] Al-Ahwal MS, Shafik YH, Al-Ahwal HM. First national survival data for colorectal cancer among Saudis between 1994 and 2004: what's next? BMC Public Health. 2013;13:73.
[8] Bakarman MA, AlGarni AM. Colorectal cancer patients in western Saudi Arabia. Outcomes and predictors for survival over a 10-years period (2002–2014). Saudi Med J. 2019;40(12):1227–34.

[9] Kuipers EJ, Grady WM, Lieberman D, Seufferlein T, Sung JJ, Boelens PG, et al. Colorectal cancer. Nat Rev Dis Primers. 2015;1:15065.
[10] Vasen HF, Tomlinson I, Castells A. Clinical management of hereditary colorectal cancer syndromes. Nat Rev Gastroenterol Hepatol. 2015;12(2):88–97.
[11] Yamagishi H, Kuroda H, Imai Y, Hiraishi H. Molecular pathogenesis of sporadic colorectal cancers. Chin J Cancer. 2016;35:4.
[12] Pathak SJ, Mueller JL, Okamoto K, Das B, Hertecant J, Greenhalgh L, et al. EPCAM mutation update: Variants associated with congenital tufting enteropathy and Lynch syndrome. Hum Mutat. 2019;40(2):142–61.
[13] Korinek V, Barker N, Morin PJ, van Wichen D, de Weger R, Kinzler KW, et al. Constitutive transcriptional activation by a beta-catenin-Tcf complex in APC-/- colon carcinoma. Science. 1997;275(5307):1784–7.
[14] Fodde R, Smits R, Clevers H. APC, signal transduction and genetic instability in colorectal cancer. Nat Rev Cancer. 2001;1(1):55–67.
[15] Bian J, Dannappel M, Wan C, Firestein R. Transcriptional Regulation of Wnt/beta-Catenin Pathway in Colorectal Cancer. Cells. 2020;9(9):2125.
[16] Flores-Hernandez E, Velazquez DM, Castaneda-Patlan MC, Fuentes-Garcia G, Fonseca-Camarillo G, Yamamoto-Furusho JK, et al. Canonical and non-canonical Wnt signaling are simultaneously activated by Wnts in colon cancer cells. Cell Signal. 2020;72:109636.
[17] Yao Q, An Y, Hou W, Cao YN, Yao MF, Ma NN, et al. Correction: LRP6 promotes invasion and metastasis of colorectal cancer through cytoskeleton dynamics. Oncotarget. 2020;11(32):3102.
[18] Yao Q, An Y, Hou W, Cao YN, Yao MF, Ma NN, et al. LRP6 promotes invasion and metastasis of colorectal cancer through cytoskeleton dynamics. Oncotarget. 2017;8(65):109632–45.
[19] Hu F, Li G, Huang C, Hou Z, Yang X, Luo X, et al. The autophagy-independent role of BECN1 in colorectal cancer metastasis through regulating STAT3 signaling pathway activation. Cell Death Dis. 2020;11(5):304.
[20] Abdulla MH, Valli-Mohammed MA, Al-Khayal K, Al Shkieh A, Zubaidi A, Ahmad R, et al. Cathepsin B expression in colorectal cancer in a Middle East population: Potential value as a tumor biomarker for late disease stages. Oncol Rep. 2017;37(6):3175–80.
[21] Gondi CS, Rao JS. Cathepsin B as a cancer target. Expert Opin Ther Targets. 2013;17(3):281–91.
[22] Bian B, Mongrain S, Cagnol S, Langlois MJ, Boulanger J, Bernatchez G, et al. Cathepsin B promotes colorectal tumorigenesis, cell invasion, and metastasis. Mol Carcinog. 2016;55(5):671–87.
[23] Marten K, Bremer C, Khazaie K, Sameni M, Sloane B, Tung CH, et al. Detection of dysplastic intestinal adenomas using enzyme-sensing molecular beacons in mice. Gastroenterology. 2002;122(2):406–14.
[24] Piawah S, Venook AP. Targeted therapy for colorectal cancer metastases: A review of current methods of molecularly targeted therapy and the use of tumor biomarkers in the treatment of metastatic colorectal cancer. Cancer. 2019;125(23):4139–47.
[25] Baskar R, Dai J, Wenlong N, Yeo R, Yeoh KW. Biological response of cancer cells to radiation treatment. Front Mol Biosci. 2014;1:24.
[26] Goodwin RA, Asmis TR. Overview of systemic therapy for colorectal cancer. Clin Colon Rectal Surg. 2009;22(4):251–6.
[27] Nath D, Banerjee P. Green nanotechnology – a new hope for medical biology. Env Toxicol Pharmacol. 2013;36(3):997–1014.
[28] Gurunathan S, Park JH, Han JW, Kim JH. Comparative assessment of the apoptotic potential of silver nanoparticles synthesized by Bacillus tequilensis and Calocybe indica in MDA-MB-231 human breast cancer cells: targeting p53 for anticancer therapy. Int J Nanomed. 2015;10:4203–22.
[29] Zhang XF, Liu ZG, Shen W, Gurunathan S. Silver nanoparticles: synthesis, characterization, properties, applications, and therapeutic approaches. Int J Mol Sci. 2016;17(9):1534.
[30] Rajan R, Huo P, Chandran K, Manickam Dakshinamoorthi B, Yun SI, Liu B. A review on the toxicity of silver nanoparticles against different biosystems. Chemosphere. 2022;292:133397.
[31] Boverhof DR, Bramante CM, Butala JH, Clancy SF, Lafranconi M, West J, et al. Comparative assessment of nanomaterial definitions and safety evaluation considerations. Regul Toxicol Pharmacol. 2015;73(1):137–50.
[32] Ferdous Z, Nemmar A. Health impact of silver nanoparticles: a review of the biodistribution and toxicity following various routes of exposure. Int J Mol Sci. 2020;21(7):2375.
[33] Thakkar KN, Mhatre SS, Parikh RY. Biological synthesis of metallic nanoparticles. Nanomedicine. 2010;6(2):257–62.
[34] Mikhailova EO. Silver nanoparticles: mechanism of action and probable bio-application. J Funct Biomater. 2020;11(4):84.
[35] Biswas A, Vanlalveni C, Adhikari PP, Lalfakzuala R, Rokhum L. Green biosynthesis, characterisation and antimicrobial activities of silver nanoparticles using fruit extract of Solanum viarum. IET Nanobiotechnol. 2018;12(7):933–8.
[36] Althurwi HN, Abdel-Kader MS, Alharthy KM, Salkini MA, Albaqami FF. Cymbopogon proximus essential oil protects rats against isoproterenol-induced cardiac hypertrophy and fibrosis. Molecules. 2020;25(8):1786.
[37] Elgamal MH, Wolff P. A further contribution to the sesquiterpenoid constituents of cymbopogon proximus. Planta Med. 1987;53(3):293–4.
[38] Avoseh O, Oyedeji O, Rungqu P, Nkeh-Chungag B, Oyedeji A. Cymbopogon species; ethnopharmacology, phytochemistry and the pharmacological importance. Molecules. 2015;20(5):7438–53.
[39] Paduch R, Kandefer-Szerszen M, Trytek M, Fiedurek J. Terpenes: substances useful in human healthcare. Arch Immunol Ther Exp. 2007;55(5):315–27.
[40] Al Hargan A, Daghestani MH, Harrath AH. Alterations in APC, BECN1, and TP53 gene expression levels in colon cancer cells caused by monosodium glutamate. Braz J Biol. 2021;83:e246970.
[41] Sekine S, Shibata T, Sakamoto M, Hirohashi S. Target disruption of the mutant beta-catenin gene in colon cancer cell line HCT116: preservation of its malignant phenotype. Oncogene. 2002;21(38):5906–11.
[42] Miethling-Graff R, Rumpker R, Richter M, Verano-Braga T, Kjeldsen F, Brewer J, et al. Exposure to silver nanoparticles induces size- and dose-dependent oxidative stress and

cytotoxicity in human colon carcinoma cells. Toxicol In Vitro. 2014;28(7):1280–9.
[43] Erdogan O, Abbak M, Demirbolat GM, Birtekocak F, Aksel M, Pasa S, et al. Green synthesis of silver nanoparticles via Cynara scolymus leaf extracts: The characterization, anticancer potential with photodynamic therapy in MCF7 cells. PLoS One. 2019;14(6):e0216496.
[44] Senthil B, Devasena T, Prakash B, Rajasekar A. Non-cytotoxic effect of green synthesized silver nanoparticles and its antibacterial activity. J Photochem Photobiol B. 2017;177:1–7.
[45] Vijayan R, Joseph S, Mathew B. Anticancer, antimicrobial, antioxidant, and catalytic activities of green-synthesized silver and gold nanoparticles using Bauhinia purpurea leaf extract. Bioprocess Biosyst Eng. 2019;42(2):305–19.
[46] Venkatesan J, Kim SK, Shim MS. Antimicrobial, antioxidant, and anticancer activities of biosynthesized silver nanoparticles using marine Algae Ecklonia cava. Nanomaterials. 2016;6(12):235.
[47] Prakash P, Gnanaprakasam P, Emmanuel R, Arokiyaraj S, Saravanan M. Green synthesis of silver nanoparticles from leaf extract of Mimusops elengi, Linn. for enhanced antibacterial activity against multi drug resistant clinical isolates. Colloids Surf B. 2013;108:255–9.
[48] Niraimathi KL, Sudha V, Lavanya R, Brindha P. Biosynthesis of silver nanoparticles using Alternanthera sessilis (Linn.) extract and their antimicrobial, antioxidant activities. Colloids Surf B. 2013;102:288–91.
[49] Ahmad R, Singh JK, Wunnava A, Al-Obeed O, Abdulla M, Srivastava SK. Emerging trends in colorectal cancer: Dysregulated signaling pathways (Review). Int J Mol Med. 2021;47(3):14.
[50] Bin-Jumah M, Al-Abdan M, Albasher G, Alarifi S. Effects of green silver nanoparticles on apoptosis and oxidative stress in normal and cancerous human hepatic cells in vitro. Int J Nanomed. 2020;15:1537–48.
[51] Kovacs D, Igaz N, Gopisetty MK, Kiricsi M. Cancer therapy by silver nanoparticles: fiction or reality? Int J Mol Sci. 2022;23(2):839.
[52] Gurunathan S, Qasim M, Park C, Yoo H, Kim JH, Hong K. Cytotoxic potential and molecular pathway analysis of silver nanoparticles in human colon cancer cells HCT116. Int J Mol Sci. 2018;19(8):2269.
[53] Acharya D, Satapathy S, Somu P, Parida UK, Mishra G. Apoptotic effect and anticancer activity of biosynthesized silver nanoparticles from marine algae chaetomorpha linum extract against human colon cancer Cell HCT-116. Biol Trace Elem Res. 2021;199(5):1812–22.
[54] Kermanizadeh A, Chauche C, Balharry D, Brown DM, Kanase N, Boczkowski J, et al. The role of Kupffer cells in the hepatic response to silver nanoparticles. Nanotoxicology. 2014;8(Suppl 1):149–54.
[55] Wen H, Dan M, Yang Y, Lyu J, Shao A, Cheng X, et al. Acute toxicity and genotoxicity of silver nanoparticle in rats. PLoS One. 2017;12(9):e0185554.
[56] Park EJ, Bae E, Yi J, Kim Y, Choi K, Lee SH, et al. Repeated-dose toxicity and inflammatory responses in mice by oral administration of silver nanoparticles. Env Toxicol Pharmacol. 2010;30(2):162–8.
[57] Dan M, Wen H, Shao A, Xu L. Silver nanoparticle exposure induces neurotoxicity in the rat hippocampus without increasing the blood-brain barrier permeability. J Biomed Nanotechnol. 2018;14(7):1330–8.
[58] Tang J, Xiong L, Zhou G, Wang S, Wang J, Liu L, et al. Silver nanoparticles crossing through and distribution in the blood-brain barrier in vitro. J Nanosci Nanotechnol. 2010;10(10):6313–7.
[59] Gires O, Pan M, Schinke H, Canis M, Baeuerle PA. Expression and function of epithelial cell adhesion molecule EpCAM: where are we after 40 years? Cancer Metastasis Rev. 2020;39(3):969–87.